Electronic Supplementary Information

Enhanced electromagnetic wave absorption property induced by void space in hollow nanoparticles

Feng Yan,[a,b,c] Jianyu Kang,[a] Shen Zhang,[a] Chunyan Li,[a] Chunling Zhu,[*b] Xitian Zhang[c] and Yujin Chen[*a]

[a] Key Laboratory of In-Fiber Integrated Optics, Ministry of Education and College of Science, Harbin Engineering University, Harbin 150001, China.

[b] College of Chemistry and Chemical Engineering, Harbin Engineering University, Harbin 150001, China.

[c] Key Laboratory for Photonic and Electronic Bandgap Materials, Ministry of Education and School of Physics and Electronic Engineering, Harbin Normal University, Harbin 150025, China.

*Corresponding authors.
Tel.: +086-0451-82519754, Fax: +086-0451-82519754
E-mail addresses: zhuchunling@hrbeu.edu.cn (C. Zhu) or chenyujin@hrbeu.edu.cn (Y. Chen).

Experimental details

Chemicals. Graphene sheets were purchased from Nanjing XFNANO Material Tech Co., Ltd. (Nanjing City, China). Cobalt acetate, nickel acetate and ammonia were purchased from Tianjin Kermel Chemical Reagent Co., Ltd. (China). Commercially available chemical reagents were used without further purification.

Synthesis of $NiCo_2O_4$-h/G composite. Graphene (24 mg) was dispersed in ethanol (72 mL) by means of ultrasonication for 20 min, and then cobalt acetate (32 mg), nickel acetate (167 mg) was added into the above mixture. After ultrasonication sonication for another 15 min, distilled water (3.6 mL) and ammonia (2 mL) were added, respectively. The mixture above was sealed and kept at 80 ^oC for 10 h under stirring. After cooling to room temperature, the black precipitate (NiCo hydroxide/G) in the solution was collected by removing the supernatant, washing with distilled water and ethanol for several times and drying through a freeze-drying process. In the second step, the NiCo hydroxide/G composite was firstly performed by thermal treatment in a tube furnace at 350^oC for 3 h under an H_2/ Ar flow, then treated at 200^oC for 3 h and 280^oC for 3 h under air atmosphere, respectively. After being cooled to room temperature, the $NiCo_2O_4$-h/G composite was obtained.

Synthesis of $NiCo_2O_4$-s/G Co_3O_4-s/G and NiO-s/G composites. $NiCo_2O_4$-s/G was obtained by directly heating the NiCo hydroxide/G in a tube furnace at 200^oC for 3 h and 280^oC for 3 h under air atmosphere with the similar conditions. Co_3O_4-s/G was synthesized by directly adding cobalt acetate (199 mg) only in the first step, and the corresponding precursor were heated in a tube furnace at 200^oC for 3 h and 280^oC for

3 h in air flow, respectively. Similarly, the NiO-s/G was synthesized by directly adding nickel acetate (199 mg) only in the first step, and the corresponding precursor were heated in a tube furnace at 200^{o}C for 3 h and 320^{o}C for 3 h in air flow under the same conditions.

Structure Characterizations. XRD data were measured by a Rigaku D/max-2600/PC with Cu Kα radiation (λ=1.5418Å). The morphology and size of samples were characterized by scanning electron microscope (Hitachi SU70) and an FEI Tecnai-F20 transmission electron microscope equipped with a Gatan imaging filter (GIF). BET surface area and pore volume were tested with a Quantachrome Instruments NOVA4000 after the composites were vacuum dried at 200℃ over 10 h. XPS analyses were carried out by using a spectrometer with Mg Kα radiation (PHI 5700 ESCA System).The binding energy was calibrated with the C 1s position of contaminant carbon in the vacuum chamber of the XPS instrument (284.6 eV).

Electromagnetic Parameters Measurements. The electromagnetic parameters of the absorbers were measured by using a vector network analyzer (Anritsu MS4644A Vectorstar) in the frequency of 2 – 18 GHz. The cylindrical sample (with 3.00 mm inner diameter, 7.00 mm outer diameter and 3.00 mm thickness) was fabricated by uniformly mixing 50 wt% of the samples with a paraffin matrix. Before measurement, the electromagnetic parameter was verified by standard Teflon sample with the same shape and size as the tested sample.

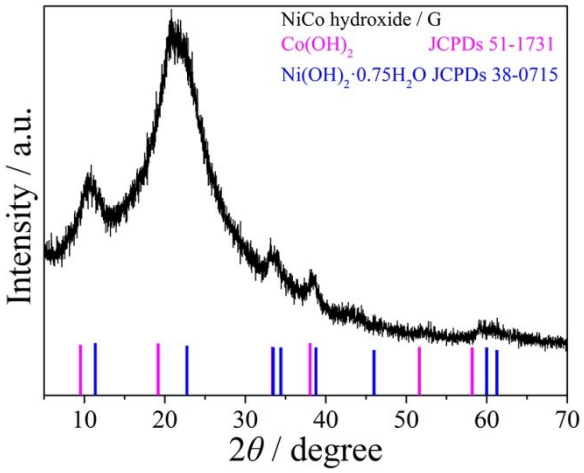

Fig. S1. The XRD pattern of NiCo hydroxide/G.

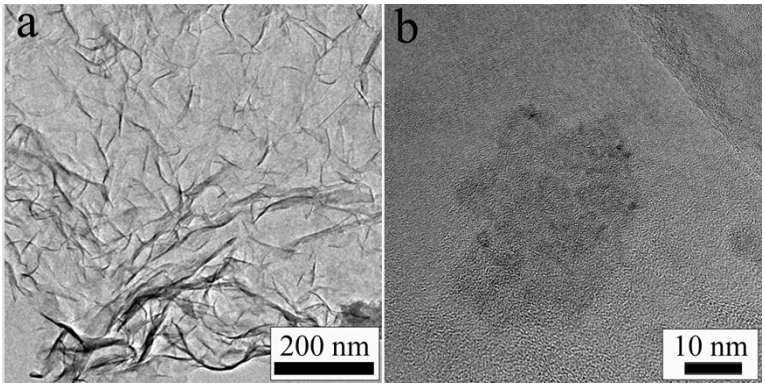

Fig. S2 The low-magnification TEM and HRTEM images of NiCo hydroxide/G.

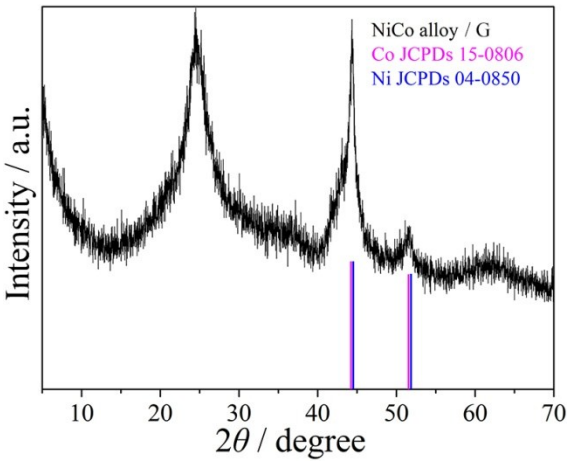

Fig. S3. The XRD pattern of NiCo alloy NPs/G.

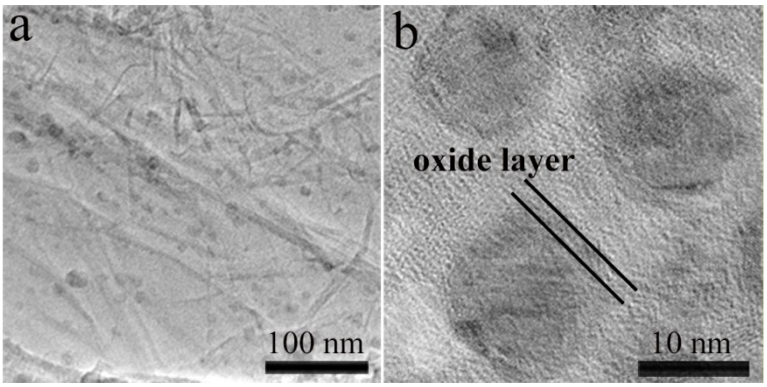

Fig. S4 The low-magnification TEM and HRTEM images of NiCo alloy NPs/G.

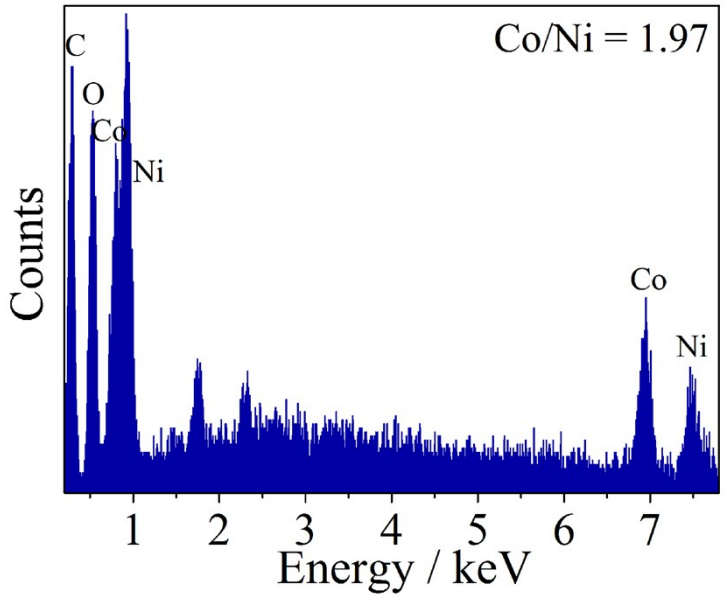

Fig. S5. EDS pattern of $NiCo_2O_4$-h/G.

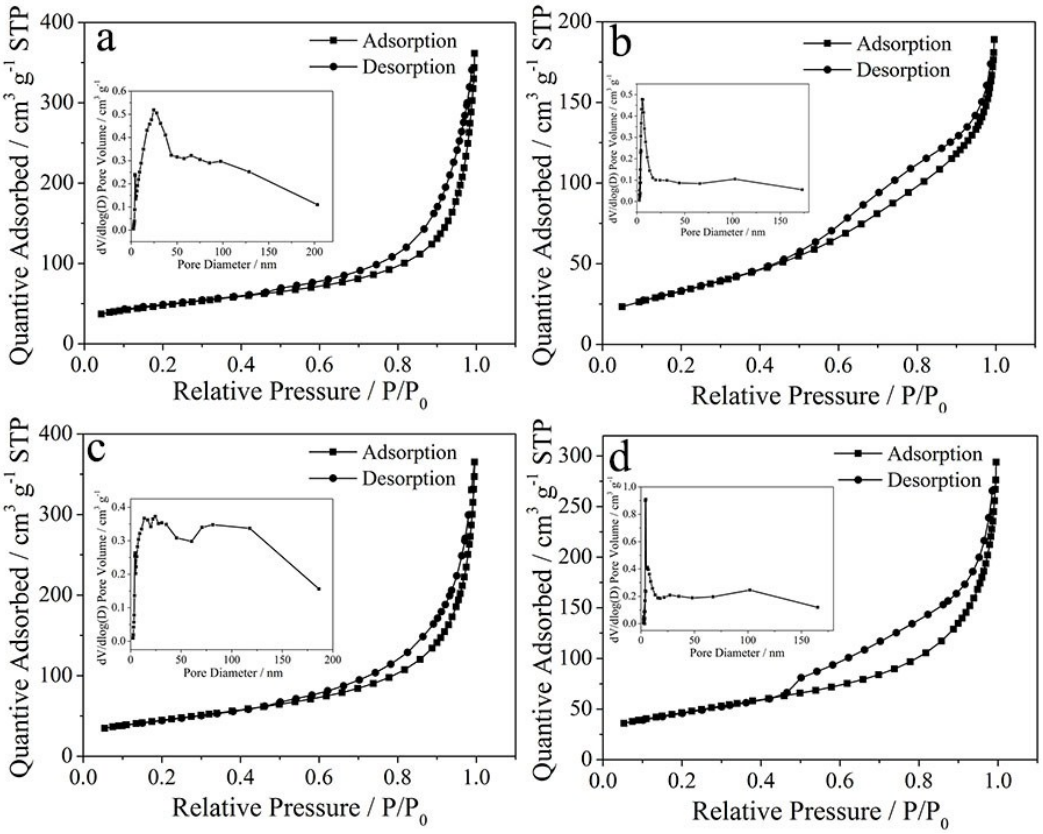

Fig. S6. Nitrogen adsorption and desorption isotherms of $NiCo_2O_4$-h/G a), $NiCo_2O_4$-s/G b), NiO-s/G c), and Co_3O_4-s/G d). The insets of a-d) show the corresponding pore-size distribution calculated by the BJH method.

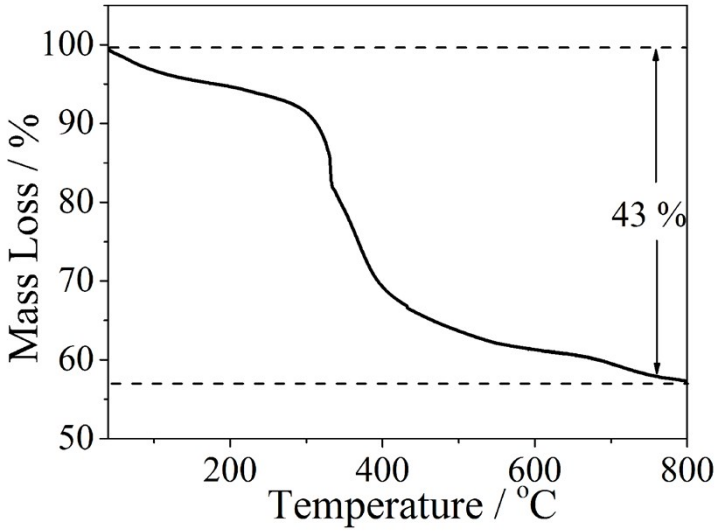

Fig. S7. The TGA of $NiCo_2O_4$-h/G.

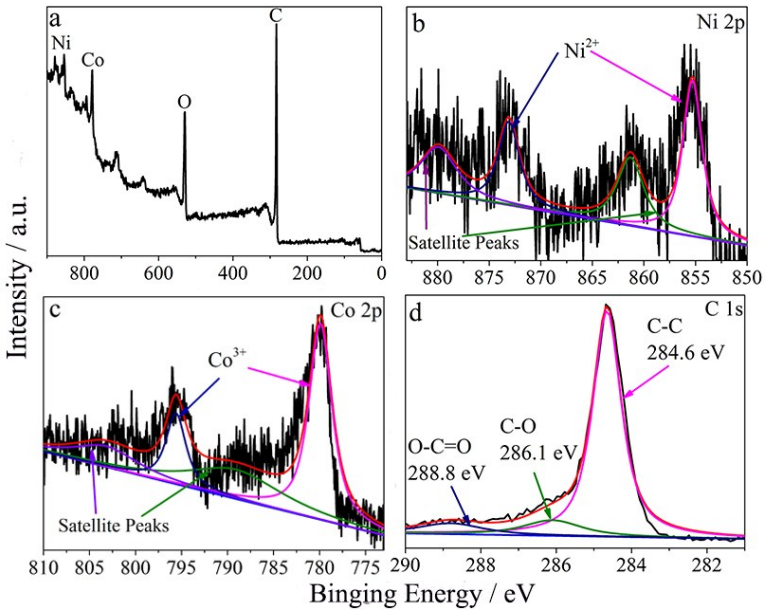

Fig. S8. The survey XPS spectrum of $NiCo_2O_4$-h/G a), the XPS spectra of Ni 2p b), Co 2p c), and C 1s in $NiCo_2O_4$-h/G d).

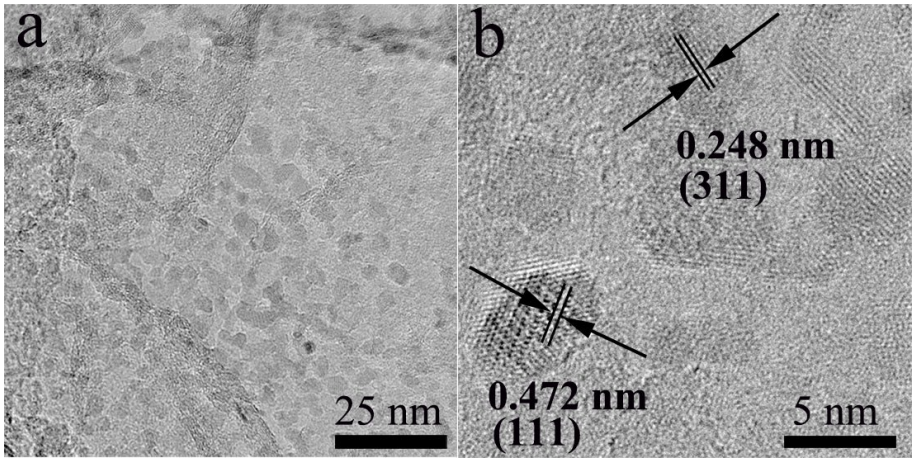

Fig. S9. The low-magnification TEM a), and HRTEM images of $NiCo_2O_4$-s/G b).

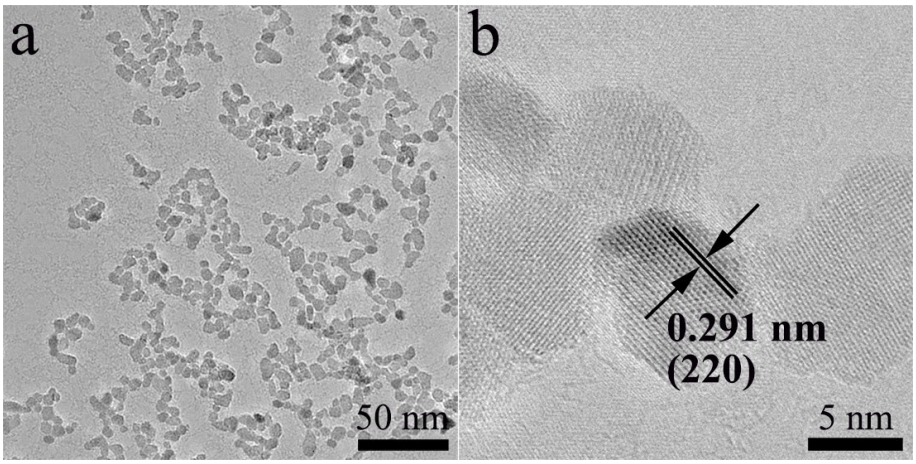

Fig. S10. The low-magnification TEM a), and HRTEM images of Co_3O_4-s/G b).

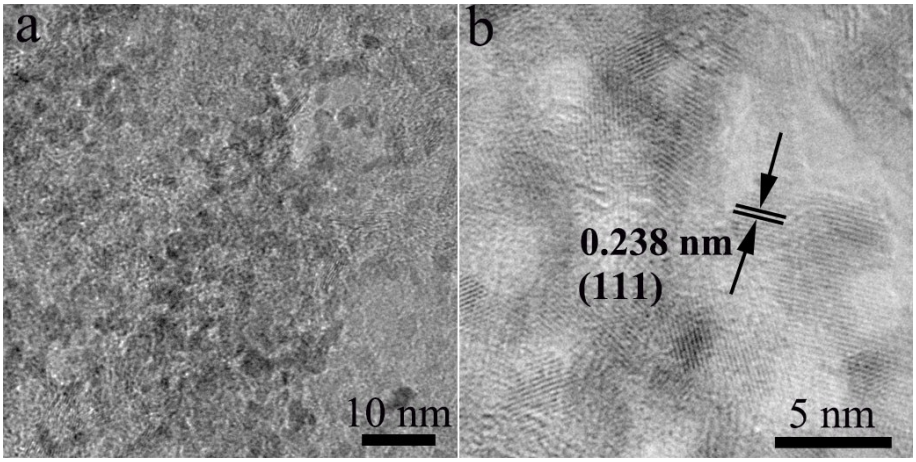

Fig. S11. The low-magnification TEM a), and HRTEM images of NiO-s/G b).

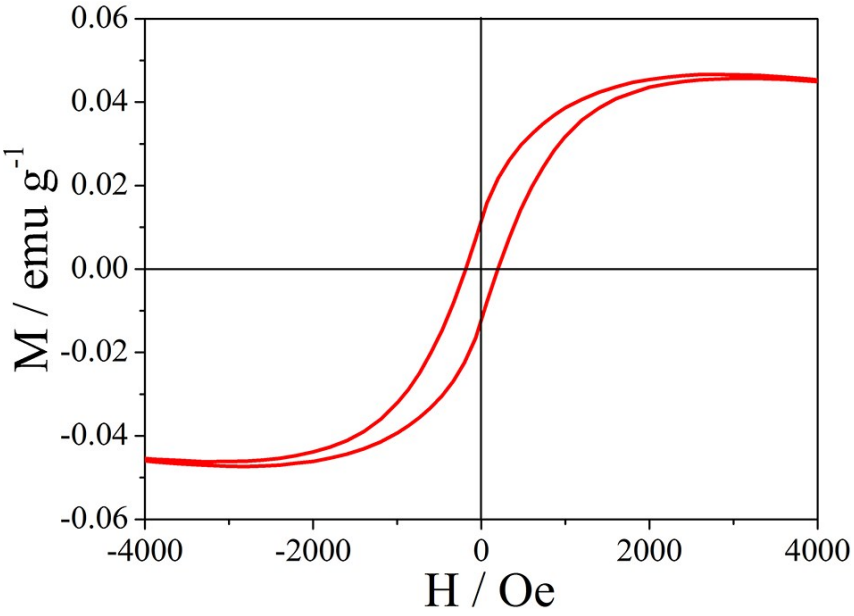

Fig. S12. Magnetization hysteresis loops of the $NiCo_2O_4$-h/G.

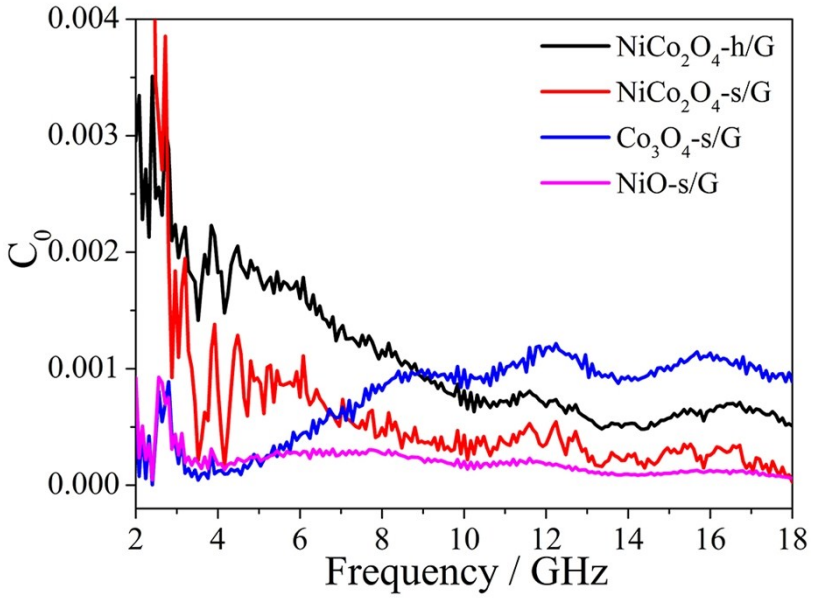

Fig. S13. The C_0–f curves of $NiCo_2O_4$-h/G, $NiCo_2O_4$-s/G, Co_3O_4-s/G and NiO-s/G.

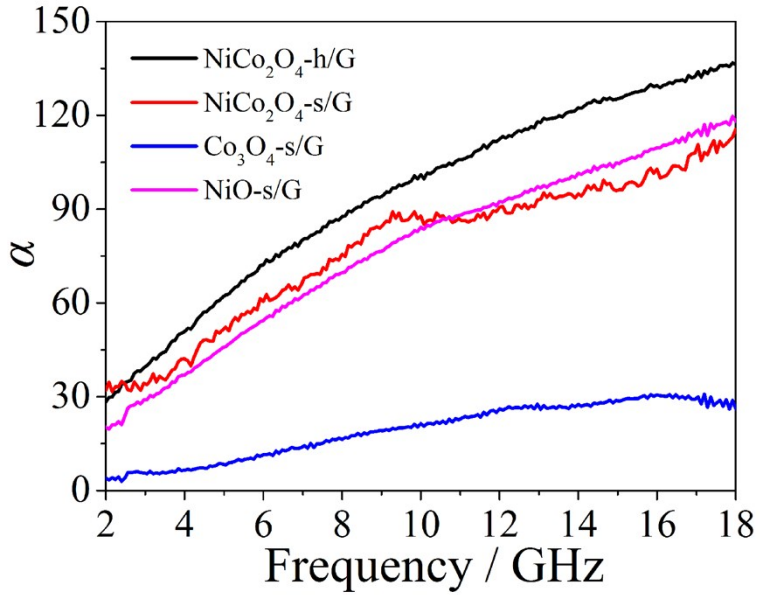

Fig. S14. The attenuation constants of $NiCo_2O_4$-h/G, $NiCo_2O_4$-s/G, Co_3O_4-s/G and NiO-s/G in the frequency of 2 – 18 GHz.

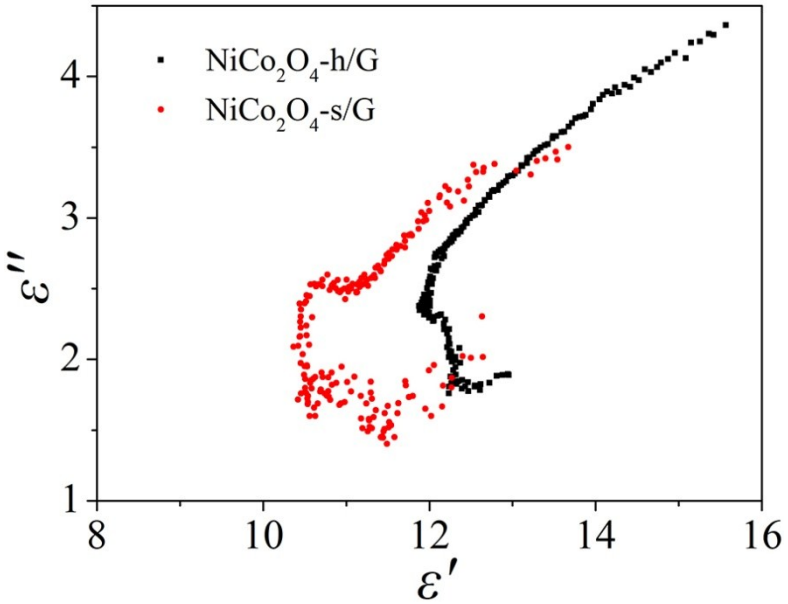

Fig. S15. The Cole-Cole semicircles of $NiCo_2O_4$-h/G and $NiCo_2O_4$-s/G.

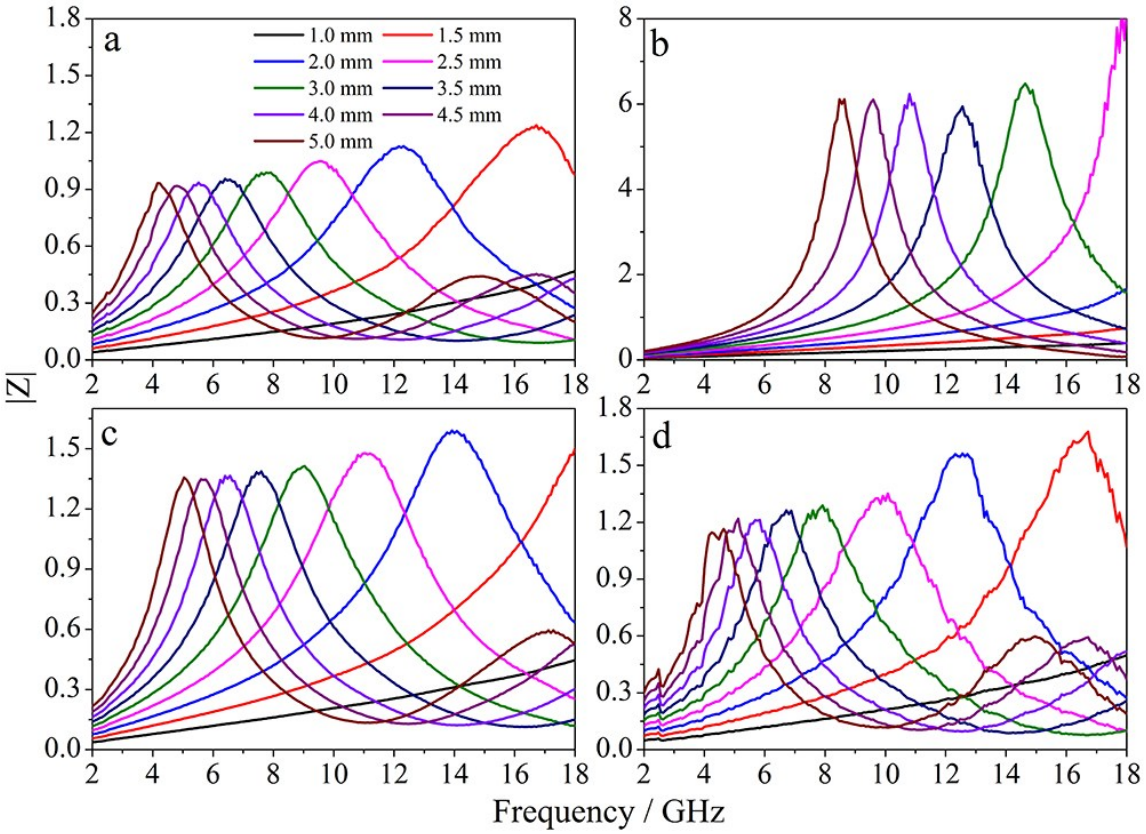

Fig. S16. The impedance matching characteristics of the $NiCo_2O_4$-h/G a), Co_3O_4-s/G b), NiO-s/G c), and $NiCo_2O_4$-s/G d).

Table S1. Comparison of EMW absorption properties of $NiCo_2O_4$-h/G with those of other reported absorbing materials.

Materials	Minimal R_L (dB)	d (mm)	Minimal R_L position (GHz)	Ref.
Hierarchical $NiCo_2O_4$	-25.5	4.0	4.5	[1]
FeCo/C nanocapsules	-29.0	5.0	~4.2	[2]
$NiFe_2O_4$-polystyrene particles	-13.0	2.0	11.5	[3]
Hollow $CoFe_2O_4$ sphere /graphene	-24.7	4.0	~5.5	[4]
Porous Co@C	-30.31	3.0	11.03	[5]
Hollow CuS microspheres	-17.8	1.5	11.5	[6]
Porous $NiCo_2O_4/Co_3O_4/NiO$	-57	4.9	5.92	[7]
Core-shell $C@NiCo_2O_4@Fe_3O_4$	-43	3.4	13.4	[8]
Ni/C microsphere	-44.5	9.5	2.6	[9]
Porous Co/C	-35.3	4.0	5.8	[10]
CoNi–C nanoparticles	-50.2	4.0	7.7	[11]
Core–shell Co@CoO fluffy microrods	-36.2	3.4	8.0	[12]
Hollow $NiCo_2O_4$/G nanoparticles	-37.3	3.0	8.0	This work

REFERENCES

1. Zhou, M.; Lu, F.; Lv, T. Y.; Yang, X.; Xia, W. W.; Shen, X. S.; He, H.; Zeng, X. H. Loss Mechanism and Microwave Absorption Properties of Hierarchical $NiCo_2O_4$ Nanomaterial. *J. Phys. D: Appl. Phys.* **2015***, 48,* 215305.
2. Han, Z.; Li, D.; Wang, H.; Liu, X. G.; Li, J.; Geng, D. Y.; Zhang, Z. D. Broadband Electromagnetic-Wave Absorption by FeCo/C Nanocapsules. *Appl. Phys. Lett.* **2009**, *95*, 023114.
3. Zhao, H. T.; Sun, X. D.; Mao, C. H.; Du, J. Preparation and Microwave–absorbing Properties of $NiFe_2O_4$-polystyrene Composites. *Physica B* **2009**, *404*, 69–72.
4. Fu, M.; Q. Jiao, Z.; Zhao, Y.; Li, H. S. Vapor Diffusion Synthesis of $CoFe_2O_4$ Hollow Sphere/Graphene Composites as Absorbing Materials. *J. Mater. Chem. A* **2014**, *2*, 735–744.
5. Wang, H.; Xiang, L.; Wei, W.; An, J.; He, J.; Gong, C. H.; Hou, Y. Efficient and Lightweight Electromagnetic Wave Absorber Derived from Metal Organic Framework-Encapsulated Cobalt Nanoparticles. *ACS Appl. Mater. Interfaces* **2017**, *9*, 42102–42110.
6. Zhao, B.; Guo, X. Q.; Zhou, Y. Y.; Su, T. T.; Ma, C.; Zhang. R. Constructing Hierarchical Hollow CuS Microspheres via a Galvanic Replacement Reaction and Their Use as Wide-band Microwave Absorbers. *CrystEngComm*, **2017**, *19*, 2178–2186.
7. Liu, X. F.; Hao, C. C.; Jiang, H.; Zeng, M.; Yu, R. H. Hierarchical $NiCo_2O_4/Co_3O_4/NiO$ Porous Composite: a Lightweight Electromagnetic Wave

Absorber with Tunable Absorbing Performance. *J. Mater. Chem. C,* **2017***, 5,* 3770–3778.

8. Wei ,S.; Wang, X. X.; Zhang, B. Q.; Yu, M. X.; Zheng, Y. W.; Wang, Y.; Liu J. Q.. Preparation of Hierarchical Core-shell C@$NiCo_2O_4$@Fe_3O_4 Composites for Enhanced Microwave Absorption Performance. *Chemical Engineering Journal* **2017,** *314,* 477–487.
9. Qiu, S.; Lyu, H. L.; Liu, J. R.; Liu, Y. Z.; Wu, N. N.; Liu, W. Facile Synthesis of Porous Nickel/Carbon Composite Microspheres with Enhanced Electromagnetic Wave Absorption by Magnetic and Dielectric Losses. *ACS Appl. Mater. Interfaces* **2016***, 8,* 20258–20266.
10. Lü, Y. Y.; Wang, Y. T.; Li, H. L.; Lin, Y.; Jiang, Z. Y.; Xie, Z. X.; Kuang, Q.; Zheng, L. S. MOF-Derived Porous Co/C Composites with Excellent Electromagnetic Wave Absorption Properties. *ACS Appl. Mater. Interfaces* **2015**, *7*, 13604–13611.
11. Li, N.; Hu, C. W.; Cao, M. H. Enhanced Microwave Absorbing Performance of CoNi Alloy Nanoparticles Anchored on a Spherical Carbon Monolith. *Phys. Chem. Chem. Phys.,* **2013***, 15,* 7685–7689.
12. Deng, J. S.; Zhang, X.; Zhao, B.; Bai, Z. Y.; Wen, S. M.; Li, S. M.; Li, S. Y.; Yang, J.; Zhang, R. Fluffy Microrods to Heighten the Microwave Absorption Properties through Tuning the Electronic State of Co/CoO. *J. Mater. Chem. C,* **2018**, *6*, 7128–7140.